

Universal scaling laws and density slopes for dark matter haloes

Zhijie (Jay) Xu,¹★

¹Physical and Computational Sciences Directorate, Pacific Northwest National Laboratory; Richland, WA 99354, USA

Accepted XXX. Received YYY; in original form ZZZ

ABSTRACT

Small scale challenges suggest some missing pieces in our current understanding of dark matter. A cascade theory for dark matter is proposed to provide extra insights, similar to the cascade phenomenon in hydrodynamic turbulence. The kinetic energy is cascaded in dark matter from small to large scales involving a constant rate ε_u ($\approx -4.6 \times 10^{-7} m^2/s^3$). Confirmed by N-body simulations, the energy cascade leads to a two-thirds law for kinetic energy v_r^2 on scale r such that $v_r^2 \propto (\varepsilon_u r)^{2/3}$. Equivalently, a four-thirds law can be established for halo density ρ_s enclosed in the scale radius r_s such that $\rho_s \propto \varepsilon_u^{2/3} G^{-1} r_s^{-4/3}$, which can be confirmed by galaxy rotation curves. Critical properties of dark matter might be obtained by identifying key constants on relevant scales. First, the largest halo scale r_l can be determined by $-u_0^3/\varepsilon_u$, where u_0 is the velocity dispersion. Second, the smallest scale r_η is dependent on the nature of dark matter. For collisionless dark matter, length scale $r_\eta \propto (-G\hbar/\varepsilon_u)^{1/3} \approx 10^{-13} m$ was found along with the mass scale $m_X \propto (-\varepsilon_u \hbar^5 G^{-4})^{1/9} \approx 10^{12} GeV$, where \hbar is the Planck constant. An uncertainty principle for momentum and acceleration fluctuations is also postulated. For self-interacting dark matter, $r_\eta \propto \varepsilon_u^2 G^{-3} (\sigma/m)^3$, where σ/m is the cross-section of interaction. On halo scale, the energy cascade leads to an asymptotic density slope $\gamma = -4/3$ for fully virialized haloes with a vanishing radial flow, which might explain the nearly universal halo density. Based on the continuity equation, halo density is analytically shown to be closely dependent on the radial flow and mass accretion, such that simulated haloes can have different limiting slopes. A modified Einasto density profile is proposed accordingly.

Key words: Dark matter flow; N-body simulations; Rotation curve; Collisionless; Self-interacting; Core-cusp; Energy cascade

CONTENTS

- 1 Introduction
- 2 The constant rate of energy cascade
- 3 The 2/3 and -4/3 laws for energy and density
- 4 Halo density slope and mean radial flow
- 5 Testing -4/3 law against rotation curves
- 6 Scales for self-interacting dark matter
- 7 Scales for collisionless dark matter
- 8 Conclusions

1 INTRODUCTION

Standard CDM (cold dark matter) paradigm of cosmology has many successes in the formation and evolution of large scale structures and the contents and states of our universe [1, 2, 3, 4]. Despite great successes, serious theoretical and observational difficulties still exist [5, 6]. Especially, CDM model predictions of structures on small scales ($<1\text{Mpc}$) are inconsistent with some observations. Examples are the core-cusp problem [7, 8], the missing satellite problem [9, 10], the too-big-to-fail problem [11, 12]. In addition, the origin of Baryonic Tully-Fishery relation (BTFR) and MOND (modified Newtonian dynamics) [13, 14, 15] is still not clear.

These small scale challenges might be related to each other [6, 16, 17] and suggest missing pieces in our current understandings.

First, the cusp-core problem describes the discrepancy between the cuspy halo density predicted by cosmological CDM only N-body simulations and the cored density inferred from observational data for dwarf galaxies. The predicted halo density exhibits a cuspy profile with inner density $\rho(r) \propto r^\gamma$, where slope γ persistently exceeds different observations [18, 19, 20, 21]. Even for the cuspy profile predicted by cosmological simulations, there seems no consensus on the exact value of asymptotic slope γ , but with a wide range between -1.0 to -1.5. Since the first prediction of $\gamma = -1.0$ in NFW profile [22], the inner density slope of simulated haloes seems to have different values from $\gamma > -1.0$ [23] to $\gamma = -1.2$ [24], and $\gamma = -1.3$ [25, 26]. To summarize, some key questions are: is there an asymptotic slope for dark matter haloes? why there exists a nearly universal density profile? and why different inner slopes γ exist in simulations?

The halo density inferred from observational data exacerbates the problem. Even the smallest predicted inner density slope from simulations is still greater than that from observations. Many solutions have been suggested to solve the cusp-core problem [27]. Within the CDM framework of collisionless dark matter, the baryonic solutions focus on different mechanisms for energy exchange between baryons and dark matter to enable a flatter inner density [28, 29, 30]. Beyond the CDM framework, the self-interacting dark matter is proposed as a potential solution [31, 32, 33]. The elastic scattering with a given cross-section facilitates the exchange of momentum and energy between dark matter particles and the formation of a flat core. Although the existence of dark matter is supported by numerous astronomical observations [34, 35], the nature and fundamental properties of

★ E-mail: zhijie.xu@pnnl.gov; zhijie.xu@hotmail.com

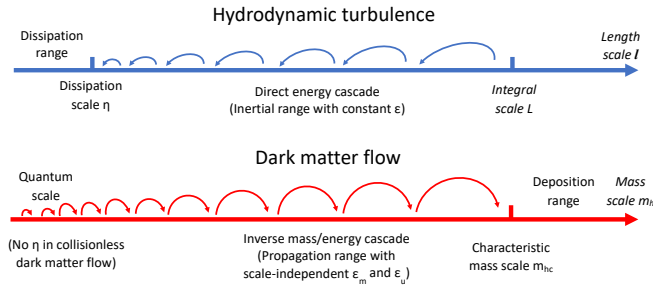


Figure 1. Schematic plot of the direct energy cascade in turbulence and the inverse mass and energy cascade in dark matter flow. Haloes merge with single mergers to facilitate a continuous mass and energy cascade to large scales. Scale-independent mass flux ε_m and energy flux ε_u are expected for haloes smaller than a characteristic mass scale (propagation range similar to the inertial range in turbulence). Mass cascaded from small scales is consumed to grow haloes at scales above the characteristic mass (the deposition range similar to the dissipation range in turbulence), where mass and energy flux become scale-dependent [40, 41, 42].

dark matter are still a big mystery. No matter collisionless or self-interacting, some key questions remain open: what are the limiting length or density scales for dark matter if exist? what is the effect of self-interaction on these scales? what are the fundamental properties (particle mass, cross-section etc.) of dark matter? Answers to these questions would be critical for identifying and detecting dark matter.

In this paper, a cascade theory for dark matter flow is proposed to provide some useful insights, similar to the cascade in hydrodynamic turbulence. Both dark matter flow and turbulence are typical non-equilibrium systems involving energy cascade as a key mechanism to continuously release energy and maximize system entropy. To grasp the key idea, we first present the cascade in turbulence that has been well-studied for many decades [36, 37, 38]. As shown in Fig. 1, turbulence consists of a collection of eddies (building blocks) on different length scale l that are interacting with each other. The classical picture of turbulence is an eddy-mediated energy cascade process, where kinetic energy of large eddies feeds smaller eddies, which feeds even smaller eddies, and so on to the smallest scale η where viscous dissipation is dominant. The direct energy cascade in turbulence can be best described by a poem [39]:

"Big whirls have little whirls, That feed on their velocity;
And little whirls have lesser whirls, And so on to viscosity."

Despite the similarities, dark matter flow exhibits many different behaviors due to its collisionless and long-range interaction nature. First, unlike the turbulence that is incompressible on all scales, dark matter flow exhibits scale-dependent flow behaviors, i.e. a constant divergence flow on small scales and irrotational flow on large scales [43]. Second, the long-range gravity requires a broad spectrum of haloes to be formed to maximize the system entropy [44]. In principle, haloes of different mass can be grouped into groups of haloes with the same mass m_h . Mass accretion facilitates a continuous mass and energy exchange between haloes groups on different mass scale m_h , i.e. an inverse mass and energy cascade (Fig. 1).

The highly localized and over-dense haloes are a major manifestation of nonlinear gravitational collapse [45, 46] and the building blocks of dark matter flow, a counterpart to "eddies" in turbulence. The halo-mediated inverse mass cascade is not present in turbulence, but exists as a local, two-way, and asymmetric process in dark matter flow [41]. The net mass transfer proceeds in a "bottom-up" fashion from small to large mass scales (inverse cascade) to allow for hierarchical structure formation. Haloes pass their mass onto larger and

larger haloes, until halo mass growth becomes dominant over the mass propagation. From this description, mass cascade can be described by a similar poem with "eddies" (or "whirls") simply replaced by "haloes":

"Little haloes have big haloes, That feed on their mass;
And big haloes have greater haloes, And so on to growth."

Energy cascade across halo groups is facilitated by the mass cascade and also a fundamental feature. Even on the halo scale, since haloes are non-equilibrium objects, energy cascade should also play a role in the abundance and internal structure of haloes [47]. In this paper, we focus on the energy cascade, its evidence from galaxy rotation curves, and its critical roles for halo internal structure and dark matter properties.

2 THE CONSTANT RATE OF ENERGY CASCADE

Particle-based N-body simulations are widely used to study the non-linear gravitational collapse of dark matter [48]. The simulation data for this work was generated from N-body simulations by Virgo consortium [49, 50]. One way to determine the constant rate of energy cascade ε_u is from a cosmic energy equation for energy evolution of dark matter flow in expanding background [51, 52, 53],

$$\frac{\partial E_y}{\partial t} + H(2K_p + P_y) = 0, \quad (1)$$

which is a manifestation of energy conservation. Here K_p is the specific (peculiar) kinetic energy, P_y is the specific potential energy in physical coordinate, $E_y = K_p + P_y$ is the total energy, $H = \dot{a}/a$ is the Hubble parameter ($Ht = 2/3$ for matter dominant universe), and a is the scale factor. In statistically steady state, Eq. (1) admits a linear solution of $K_p = -\varepsilon_u t$ and $P_y = 1.4\varepsilon_u t$ (see Fig. 2) such that ε_u can be found as,

$$\varepsilon_u = -\frac{K_p}{t} = -\frac{3}{2} \frac{u^2}{t} = -\frac{3}{2} \frac{u_0^2}{t_0} = -\frac{9}{4} H_0 u_0^2 \approx -4.6 \times 10^{-7} \frac{m^2}{s^3}, \quad (2)$$

where $u_0 \equiv u(t = t_0) \approx 354.6 \text{ km/s}$ is the one-dimensional velocity dispersion of all dark matter particles and t_0 is the present age of universe (13.8 billion years). The constant ε_u represents the rate of energy cascade across different scales. The negative value $\varepsilon_u < 0$ reflects the direction (inverse) from small to large mass scales.

3 THE 2/3 AND -4/3 LAWS FOR ENERGY AND DENSITY

To develop statistical theory of dark matter flow on all scales, different statistical measures can be introduced including the correlation, structure, dispersion functions, and power spectrum for density, velocity and potential fields [43]. Among different measures, structure functions are of particular interest that describes how energy is distributed and transferred across different length scales. For a pair of particles at two different locations \mathbf{x} and \mathbf{x}' with velocity \mathbf{u} and \mathbf{u}' , the second order longitudinal structure function S_2^{lp} (pairwise velocity dispersion in cosmology terms) is defined as

$$S_2^{lp}(r, t) = \langle (\Delta u_L)^2 \rangle = \langle (u'_L - u_L)^2 \rangle, \quad (3)$$

where $u_L = \mathbf{u} \cdot \hat{\mathbf{r}}$ and $u'_L = \mathbf{u}' \cdot \hat{\mathbf{r}}$ are two longitudinal velocities. The distance $r \equiv |\mathbf{r}| = |\mathbf{x}' - \mathbf{x}|$ and the unit vector $\hat{\mathbf{r}} = \mathbf{r}/r$ (see Fig. 3). For a given scale r , all particle pairs with the same separation r can be identified in N-body simulation. The particle position and velocity

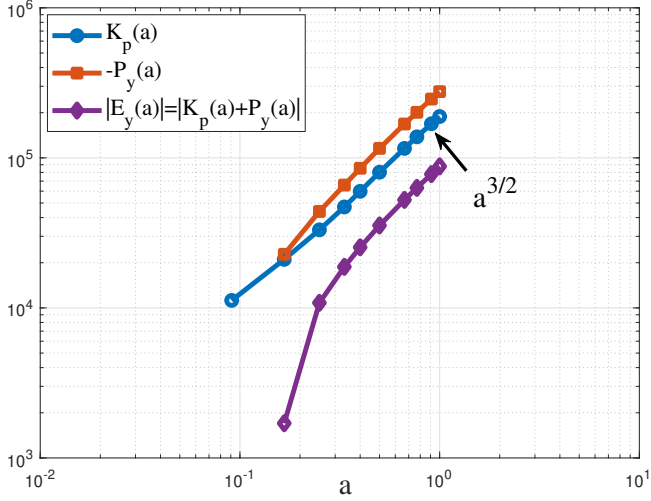


Figure 2. The time variation of kinetic and potential energies from N -body simulation. Both exhibit a power-law scaling with scale factor a , i.e. K_p and $P_y \propto a^{3/2} \propto \varepsilon_u t$. The proportional constant ε_u is estimated in Eq. (2).

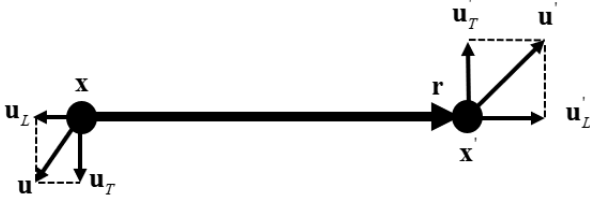


Figure 3. Sketch of longitudinal and transverse velocities, where \mathbf{u}_T and \mathbf{u}'_T are transverse velocities at two locations \mathbf{x} and \mathbf{x}' . \mathbf{u}_L and \mathbf{u}'_L are two longitudinal velocities.

data were recorded to compute the structure function in Eq. (3) by averaging over all pairs with the same r (i.e. a pairwise average).

In incompressible flow, the structure function has a small scale limit $\lim_{r \rightarrow 0} S_2^{lp} = 0$ because of $\mathbf{u}_L \approx \mathbf{u}'_L$ due to the viscous force.

However, in dark matter flow, $\lim_{r \rightarrow 0} S_2^{lp} = 2u^2 \neq 0$ due to the collisionless nature [54, 55], where u^2 is velocity dispersion in Eq. (2). The pair of particles with a sufficiently small r is more likely from the same halo, while different pairs can be from different haloes. Kinetic energy of particle pairs on scale r includes contributions from both the relative motion of two particles and the motion of haloes that particle pair resides in. The kinetic energy from the motion of haloes ($2u^2$) is relatively the same for different pairs. Kinetic energy involved in the energy cascade should be the part due to the relative motion. Since the original structure function (pairwise dispersion) $S_2^{lp}(r)$ includes the total kinetic energy on scale r , a reduced structure function $S_{2r}^{lp}(r) = S_2^{lp} - 2u^2$ can be introduced to take the common part out and include only the part from relative motion with the right limit $\lim_{r \rightarrow 0} S_{2r}^{lp} = 0$. This description indicates that $S_{2r}^{lp}(r)$ should be determined by and only by ε_u (m^2/s^3), gravitational constant G ($m^3/kg \cdot s^2$), and scale r . By a simple dimensional analysis, this reduced structure function must follow a two-thirds law, i.e. $S_{2r}^{lp}(r) \propto (-\varepsilon_u)^{2/3} r^{2/3}$.

Figure 4 plots the variation of S_{2r}^{lp} with scale r at $z=0$ from N -body

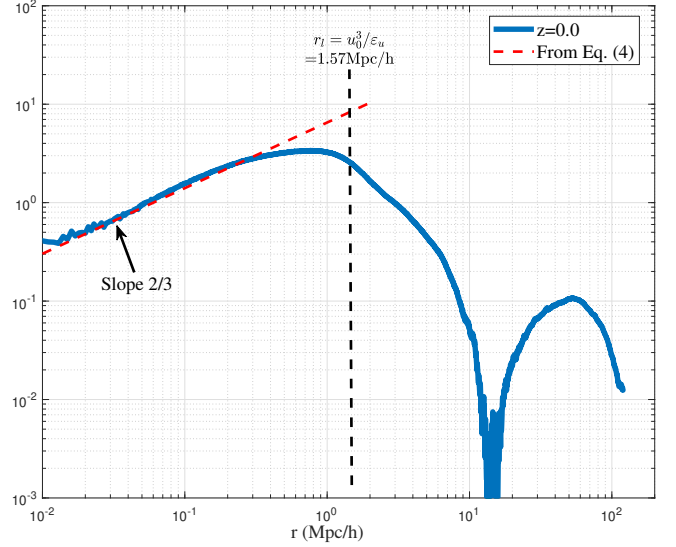


Figure 4. The variation of reduced second order structure function $S_{2r}^{lp}(r)$ with comoving scale r at $z=0$. Structure function is normalized by the velocity dispersion u^2 . A two-thirds law, i.e. $\propto (-\varepsilon_u)^{2/3} r^{2/3}$ can be clearly identified on small scale below a length scale $r_l = -u_0^3/\varepsilon_u$, where inverse energy cascade is established with a constant energy flux $\varepsilon_u < 0$. The model from Eq. (4) is also presented for comparison.

simulations. The range $S_{2r}^{lp} \propto (-\varepsilon_u)^{2/3}$ can be clearly identified below a critical length scale $r_l = -u_0^3/\varepsilon_u$. This range is formed due to the formation of haloes and inverse energy cascade. On small scale, S_{2r}^{lp} (kinetic energy) should finally read

$$S_{2r}^{lp}(r) = a^{3/2} \beta_2^* (-\varepsilon_u)^{2/3} r^{2/3}, \quad (4)$$

where the proportional constant $\beta_2^* \approx 9.5$ can be found from Fig. 4.

Since S_{2r}^{lp} represents the kinetic energy of relative motion on scale r , a different form of the two-thirds law (Eq. (4)) can be obtained. By introducing a typical velocity v_r on a given scale r ,

$$v_r^2 = S_{2r}^{lp}(r) / (2^{2/3} \beta_2^* a^{3/2}), \quad (5)$$

the two-thirds law in Eq. (4) can be equivalently written as,

$$-\varepsilon_u = \frac{2v_r^2}{r} v_r = a_r v_r = \frac{2v_r^2}{r/v_r} = \frac{2v_r^3}{r}, \quad (6)$$

where a_r is the scale of acceleration. Equation (6) also describes the cascade of kinetic energy in the inner halo region ($r < r_s$, where r_s is the scale radius). The kinetic energy v_r^2 on scale r is cascaded to large scale during a turnaround time of $t_r = r/v_r$. Combining Eq. (6) with the virial theorem $Gm_r/r \propto v_r^2$ on scale r , we can easily obtain the typical mass m_r (enclosed within r), density ρ_r , velocity v_r , and time t_r on scale r , all determined by ε_u , G , and r :

$$m_r = \alpha_r \varepsilon_u^{2/3} G^{-1} r^{5/3} \quad \text{and} \quad \rho_r = \beta_r \varepsilon_u^{2/3} G^{-1} r^{-4/3}, \quad (7)$$

$$v_r \propto (-\varepsilon_u)^{1/3} \quad \text{and} \quad t_r \propto (-\varepsilon_u)^{-1/3} r^{2/3},$$

where α_r and β_r are two numerical constants. The predicted five-thirds law for mass m_r enclosed in scale r can be directly tested by N -body simulations. In this work, the large scale cosmological simulation Illustris (Illustris-1-Dark) was selected for comparison [56]. Figure 5 presents the variation of enclosed mass m_r with scale r at different redshift z for all haloes with a given mass m_h . Results from ref. [57] are also presented for comparison. Both results confirm

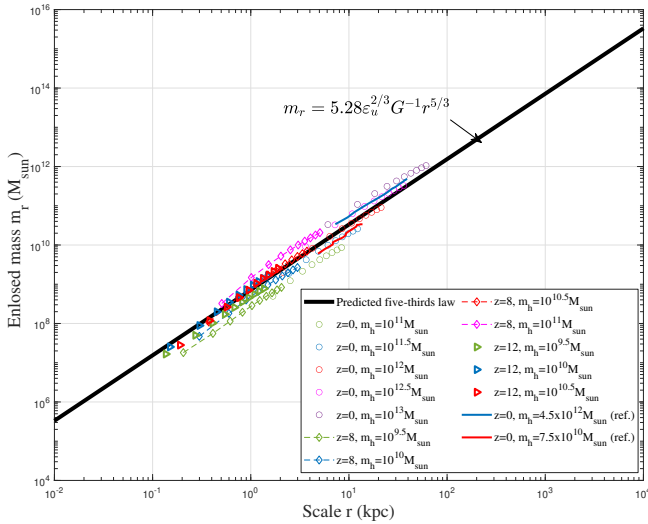


Figure 5. The variation of enclosed mass m_r with scale r at different redshift from Illustris simulation. For all haloes with a given mass m_h , the average scale radius r_s is calculated. The average enclosed mass m_r is computed for different scale r from $r = 0.1r_s$ to $r = r_s$ with an increment of $0.1r_s$. Solid blue and red lines are results from ref. [57]. Both results confirm the predicted five-thirds law in Eq. (7).

the predicted five-thirds law in Eq. (7). Next, the predicted four-thirds law $\rho_r(r) \propto r^{-4/3}$ for mean density enclosed in scale r can be directly tested by data from galaxy rotation curves (see Fig. 6).

4 HALO DENSITY SLOPE AND MEAN RADIAL FLOW

On small scale, inner halo region is assumed to be fully virialized for Eq. (7) to be valid. A vanishing radial flow u_r is expected from the stable clustering hypothesis, i.e. no net stream motion in physical coordinate along radial direction [43, 58]. With $u_r \equiv 0$, there is no mass, momentum, and energy exchanges between different spherical shells. However, simulated haloes are non-equilibrium dynamic objects that might not be fully virialized, whose internal structure should be dependent on the radial flow. The relation we'll develop in this section might be useful for core/cusp controversy.

Since halo density models often involve a scale radius r_s (the length scale of a halo), we may introduce a reduced spatial-temporal variable $x = r/r_s(t) = c(t)r/r_h(t)$, where $c \equiv c(t)$ is halo concentration and $r_h(t)$ is the virial size for halo of mass $m_h(t)$. Derivatives with respect to t and r can be derived using the chain rule,

$$\frac{\partial}{\partial t} = \frac{\partial}{\partial x} \frac{\partial x}{\partial t} = -\frac{x}{t} \frac{\partial \ln r_s}{\partial \ln t} \frac{\partial}{\partial x} \quad \text{and} \quad \frac{\partial}{\partial r} = \frac{\partial}{\partial x} \frac{\partial x}{\partial r} = \frac{1}{r_s} \frac{\partial}{\partial x}. \quad (8)$$

A general function $F(x)$ can be introduced such that the mass $m_r(r, t)$ enclosed in radius r and halo density $\rho_h(r, t)$ can all be expressed in terms of function $F(x)$,

$$m_r(r, t) = m_h(t) \frac{F(x)}{F(c)}, \quad (9)$$

$$\rho_h(r, t) = \frac{1}{4\pi r^2} \frac{\partial m_r(r, t)}{\partial r} = \frac{m_h(t)}{4\pi r_s^3} \frac{F'(x)}{x^2 F(c)}.$$

The time derivative of $\rho_h(r, t)$ can be obtained from Eq. (9),

$$\frac{\partial \rho_h(r, t)}{\partial t} = \frac{1}{4\pi r^2} \frac{\partial^2 m_r(r, t)}{\partial r \partial t}. \quad (10)$$

The mass continuity equation for a spherical halo simply reads,

$$\frac{\partial \rho_h(r, t)}{\partial t} + \frac{1}{r^2} \frac{\partial [r^2 \rho_h(r, t) u_r(r, t)]}{\partial r} = 0, \quad (11)$$

where $u_r(r, t)$ is the mean radial flow velocity. From Eqs. (10) and (11), the enclosed mass m_r is related to the radial flow as

$$\frac{\partial m_r(r, t)}{\partial t} = -4\pi r^2 u_r(r, t) \rho_h(r, t). \quad (12)$$

With m_r and ρ_h from Eq. (9), the radial flow u_r simply reads

$$u_r = -\frac{1}{4\pi r^2} \frac{\partial \ln m_r}{\partial \ln t} \frac{m_r(r, t)}{\rho_h(r, t)} = -\frac{r_s(t)}{t} \frac{\partial \ln m_r}{\partial \ln t} \frac{F(x)}{F'(x)}. \quad (13)$$

While from Eq. (9) for m_r , we have

$$\frac{\partial \ln m_r}{\partial \ln t} = \frac{\partial \ln m_h}{\partial \ln t} - \frac{x F'(x)}{F(x)} \frac{\partial \ln r_s}{\partial \ln t} - \frac{c F'(c)}{F(c)} \frac{\partial \ln c}{\partial \ln t}. \quad (14)$$

Substituting Eq. (14) into Eq. (13), the normalized radial flow u_h reads

$$u_h(x) = u_r \frac{t}{r_s} = \left[x \frac{\partial \ln r_s}{\partial \ln t} + \left(\frac{\partial \ln F(c)}{\partial \ln t} - \frac{\partial \ln m_h}{\partial \ln t} \right) \frac{F(x)}{F'(x)} \right]. \quad (15)$$

For fast growing haloes in their early stage with a constant concentration $c = 3.5$ and scale radius $r_s(t) \propto m_h(t) \propto t$, using Eq. (15), the cored density profiles (pISO, Einasto, etc. with $F(x) \propto x^3$ in Eqs. (19) and (20)) lead to $u_h = 2x/3$ for small x , while cuspy density profile (NFW with $F(x) \propto x^2$ in Eq. (20)) leads to $u_h = x/2$ for small x . Taking the derivative in Eq. (15) and combining with Eq. (9), the density slope γ can be obtained exactly as,

$$\gamma = \frac{\partial \ln \rho_h}{\partial \ln x} = \frac{\frac{\partial u_h}{\partial x} + \frac{\partial \ln m_r(r_s, t)}{\partial \ln t} - \frac{\partial \ln r_s}{\partial \ln t}}{\frac{\partial \ln r_s}{\partial \ln t} - \frac{u_h}{x}} - 2. \quad (16)$$

Clearly, the spatial variation of slope γ comes from the radial flow u_h , while the time variation of γ comes from $r_s(t)$ and $m_r(r_s, t)$ due to mass accretion. For fully virialized haloes or the virialized inner core, we should have $u_h \equiv 0$ such that the asymptotic slope γ reads

$$\gamma = \frac{\partial \ln \rho_h}{\partial \ln x} = \frac{\partial \ln m_r(r_s, t)}{\partial \ln r_s} - 3. \quad (17)$$

On halo scale, energy cascade with a constant rate ϵ_u is valid for all scales $r \leq r_s$. Taking the enclosed mass $m_r(r_s)$ as the mass scale in Eq. (7), we found $m_r(r_s) \propto r_s^{5/3}$. For fully virialized haloes with $u_h \equiv 0$, slope $\gamma = -4/3$ or a cuspy density $\rho_h(r) \propto r^{-4/3}$ can be obtained from Eq. (16). Therefore, fully virialized haloes should have universal cuspy density profiles due to energy cascade. In other words, simulated haloes might have different slope γ due to nonzero radial flow and different mass accretion rate (Eq. (16)).

The baryonic feedback provides potential mechanisms to enhance the gradient of u_h (deformation rate) in Eq. (16) and flatten the inner density. To better illustrate, we can approximate Eq. (16) in the core region as:

$$\gamma \approx \frac{\frac{\partial \ln m_r(r_s)}{\partial \ln r_s}}{1 - \mu} - 3, \quad \mu = \frac{\partial u_h}{\partial x} \left/ \frac{\partial \ln r_s}{\partial \ln t} \right. \approx \frac{u_h}{x} \left/ \frac{\partial \ln r_s}{\partial \ln t} \right. \quad (18)$$

Here dimensionless number μ represents the competition between radial flow and halo mass accretion, i.e. the deformation rate normalized by the rate of change in halo core size. The exponent $m = \partial \ln r_s / \partial \ln t$ decreases with time and increases with halo size to $m \approx 1$ for large haloes. From scaling laws for m_r in Eq. (7), $m_r(r_s) \propto r_s^{5/3}$. From Eq. (18), strong supernova-driven outflows in interstellar medium may lead to a non-zero radial outflow u_h of dark

matter or a greater μ such that core density becomes flatter from Eq. (18). This effect should be greater in smaller haloes due to smaller exponent m . Haloes should also be large enough for sufficient fraction of baryons converted into stars to allow feedback. Density cores are only developed in a certain range mass of haloes (10^{10} to $10^{11} M_\odot$), as confirmed by cosmological simulations [59].

Finally, since $u_h(x=0) \equiv 0$, there exists an asymptotic slope γ for simulated haloes for small $x \rightarrow 0$ that is dependent on the local gradient of u_h around $x=0$ (see Eq. (16)). Therefore, a better density profile can be proposed for simulated haloes (see [47] for details)

$$\rho_h(r) = \rho_0 x^\gamma \exp\left(-\frac{2}{\alpha} x^\alpha\right), \quad (19)$$

$$F(x) = \Gamma\left(\frac{3+\gamma}{\alpha}\right) - \Gamma\left(\frac{3+\gamma}{\alpha}, \frac{2}{\alpha} x^\alpha\right).$$

Here ρ_0 and α are density and shape parameters and slope $\gamma < 0$. Different simulated haloes might have different slope γ due to different behavior of radial flow u_h at small x and halo mass accretion.

5 TESTING -4/3 LAW AGAINST ROTATION CURVES

Next, the predicted four-thirds law in Eq. (7) ($\rho_r(r_s) \propto r_s^{-4/3}$) is tested against galaxy rotation curves that contain important information for dark matter haloes. In practice, rotational curves can be first decomposed into contributions from different mass components. Model parameters for halo density (scale radius r_s and density scale ρ_0) are obtained by fitting to the decomposed rotation curve. In this work, we use three sources of galaxy rotation curves,

- (i) SPARC (Spitzer Photometry & Accurate Rotation Curves) including 175 late-type galaxies [60, 61];
- (ii) DMS (DiskMass Survey) including 30 spiral galaxies [62];
- (iii) SOFUE (compiled by Sofue) with 43 galaxies [63].

The mass modeling of galaxies is always challenging because of the uncertainties in the stellar mass-to-light ratio γ . Both the DiskMass Survey (DMS) and stellar population synthesis models (SPS) suggest an almost constant γ in near-infrared band for galaxies of different masses and morphologies [60]. Wang and Chen removed the SPARC galaxies that have a bulge component to improve the fitting quality because of different mass-to-light ratio between the bulge and the disk [64]. For SPARC sample used in this work, 32 galaxies with significant bulges adopt $\gamma_{bul} = 1.4 \gamma_{disk}$ as suggested by SPS models.

For pseudo-isothermal (pISO) and NFW density, we have

$$\rho_{pISO} = \frac{\rho_0}{1+x^2}, \quad F(x) = x - \arctan(x) \approx \frac{x^3}{3}, \quad (20)$$

$$\rho_{NFW} = \frac{\rho_0}{x(1+x)^2}, \quad F(x) = \log(1+x) - \frac{x}{(1+x)} \approx \frac{x^2}{2},$$

where ρ_0 is a density parameter. From Eq. (9), halo density at r_s is

$$\rho_h(r_s) = \rho_h(x=1) = \bar{\rho}_h \frac{c^3 F'(1)}{3F(c)} = \Delta_c \rho_{crit} \frac{c^3 F'(1)}{3F(c)}, \quad (21)$$

where $\bar{\rho}_h$ is the mean halo density. In this work, $\Delta_c = 200$ and critical density $\rho_{crit} = 3H_0^2/8\pi G = 10^{-26} \text{ kg/m}^3$. Using Eqs. (20) and (21), concentration c can be obtained from fitted model parameter ρ_0 . The mean density within r_s (density scale ρ_s) now reads

$$\rho_s(r_s) = \frac{m_r(r_s)}{4\pi r_s^3/3} = \frac{F(1)c^3}{F(c)} \bar{\rho}_h = \frac{F(1)c^3}{F(c)} \Delta_c \rho_{crit}, \quad (22)$$

Figure 6 presents the variation of typical density ρ_s with scale

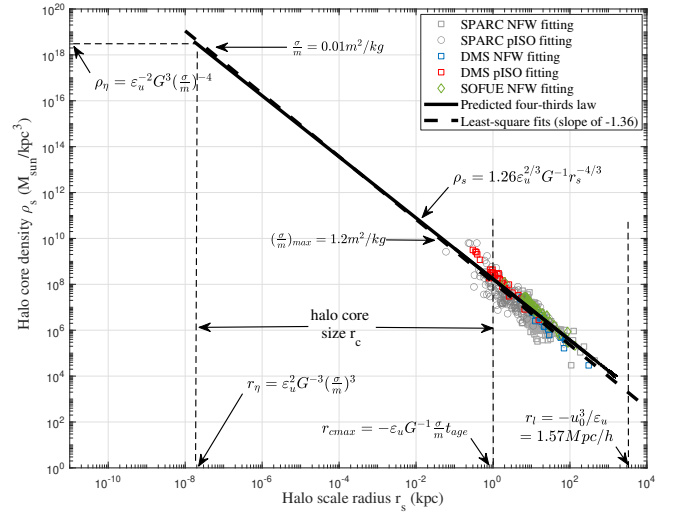


Figure 6. The predicted -4/3 law tested against actual data from galaxy rotation curves. Good agreement confirms the existence of inverse energy cascade with a constant rate ϵ_u . The self-interacting dark matter model should modify the lowest size r_η and maximum density ρ_η determined by the cross-section σ/m , below which no coherent structure can exist. The largest possible core size r_{cmax} due to self-interaction is determined by the age of haloes t_{age} . The largest scale r_l is determined by the velocity dispersion u_0 and ϵ_u .

r_s obtained from three different sources of galaxy rotation curves. Strong correlation exists between core density and scale radius with a Pearson correlation coefficient of -0.91. The four-thirds law (Eq. (7)) is also plotted for comparison with coefficients $\beta_r = 1.26$ and $\alpha_r = 5.28$ obtained from these data. The black dash line shows the least-square fit to data from all 248 galaxies with the best slope of -1.36 ± 0.05 that is very close to -4/3. The R-square value (the percentage of data variation that can be explained by model) of the fit is 0.82 with root-mean-square scatter of all data around 0.3dex. Previous studies for the scaling between halo central density and core radius have different slopes for different model fits. A constant surface density ($\rho_s r_s = \text{const}$ or $\rho_s \propto r_s^{-1.04}$) was first noticed from 55 rotation curves of spiral galaxies [65] for isothermal (ISO) fits. While slope becomes -1.20 for pseudo-isothermal (pISO) fits in the same study. Spano et al. also found a slope of -0.93 for ISO fits and -1.0 for NFW fits based on the data from 36 spiral galaxies with central density across three orders [66]. Some studies also suggest a non-constant surface density ($\rho_s r_s \neq \text{const}$). Examples are the slope of -2 [67] based on 40 spiral galaxies with core density across three orders. A slope of -1.46 was also found in galaxy cluster [68] that is close to this work.

In this work, we proposed a theory for the existence of such scaling laws. Dark matter haloes obtained from rotation curves follow the predicted four-thirds law across 6 orders in both size and density. Equivalently, the inner cuspy density $\rho_h \propto r^{-4/3}$ for virialized haloes with a vanishing radial flow is also confirmed by this plot or from Eq. (17). This plot also confirms the existence of a constant rate of cascade ϵ_u below the largest halo scale r_l . Other relevant quantities (density, pressure, energy etc.) on scale r_l are similarly determined by constants ϵ_u , G , and u_0 [69].

Finally, we can choose the circular velocity at r_s as the typical velocity $v_s = \sqrt{G m_r(r_s)/r_s}$ such that $-\epsilon_u = v_s^3/(\gamma_s r_s)$ (from Eq. (7)). Figure 7 presents the rate of energy cascade ϵ_u obtained from three sources of galaxy rotation curves with $\gamma_s = 6.83$. The disper-

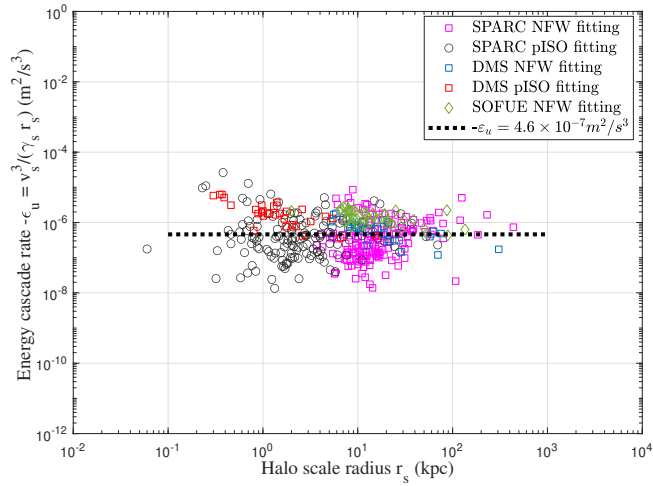


Figure 7. The constant rate of inverse energy cascade ε_u from galaxy rotation curve data. The dispersion in data might come from the spatial intermittence of energy cascade. Dwarf galaxy tends to have smaller ε_u , consistent with its density profile [47].

sion in data might come from the spatial intermittence of energy cascade such that haloes in different local environment may have slightly different ε_u .

6 SCALES FOR SELF-INTERACTING DARK MATTER

To solve the core-cusp problem, one option is the self-interacting dark matter (SIDM) model, where the cascade theory can be used to determine relevant scales. The cross-section σ/m of self-interaction should introduce additional scales r_η , ρ_η , and m_η (see Fig. 6), beyond which no structure can be formed due to self-interaction. These scales can be obtained by requiring at least one scatter per particle during the typical time t_r , i.e. $\rho_r(\sigma/m)v_r t_r = 1$ in Eq. (7). Combine this with the virial theorem and constant energy cascade in Eq. (6), the length scale r_η , density scale ρ_η , and mass scale m_η are all determined by ε_u , G , and σ/m (see Fig. 6 and Eq. (23)),

$$\begin{aligned} r_\eta &= \varepsilon_u^2 G^{-3} (\sigma/m)^3, & m_\eta &= \varepsilon_u^4 G^{-6} (\sigma/m)^5, \\ \rho_\eta &= \varepsilon_u^{-2} G^3 (\sigma/m)^{-4} \end{aligned} \quad (23)$$

From Eq. (23), the upper limit of cross section can be estimated as,

$$\frac{\sigma}{m} \leq \left(\frac{r_\eta}{1 \text{ kpc}} \right)^{\frac{1}{3}} \frac{G(1 \text{ kpc})^{1/3}}{\varepsilon_u^{2/3}} = 35.1 \frac{\text{cm}^2}{g} \left(\frac{r_\eta}{1 \text{ kpc}} \right)^{\frac{1}{3}}. \quad (24)$$

From galaxy rotation curves with a maximum core density around $\rho_\eta \approx 10^{10} M_{\text{sun}}/(kpc)^3$ and $r_\eta \approx 0.04 \text{ kpc}$ (Fig. 6), we can safely estimate the upper limit of $\sigma/m \leq 12 \text{ cm}^2/g$ from Eq. (24). High resolution rotation curves for dwarf galaxies should provide more stringent constraints on the cross-section by determining the smallest length scale r_η . For comparison, the first constraint using colliding galaxy clusters found that $\sigma/m < 5 \text{ cm}^2/g$ [70]. Analysis performed on the Bullet Cluster leads to an upper limit of $\sigma/m < 4 \text{ cm}^2/g$ from MACS J0025.4-1222 [71] and $\sigma/m < 7 \text{ cm}^2/g$ from DLSC J0916.2+2951 [72]. More stringent constraint was also obtained from Bullet Clusters 1E 0657-56 with $\sigma/m < 2 \text{ cm}^2/g$ [73].

In addition, due to self-interaction, dark matter halo should have an isothermal core with a maximum core size r_{cmax} by requiring

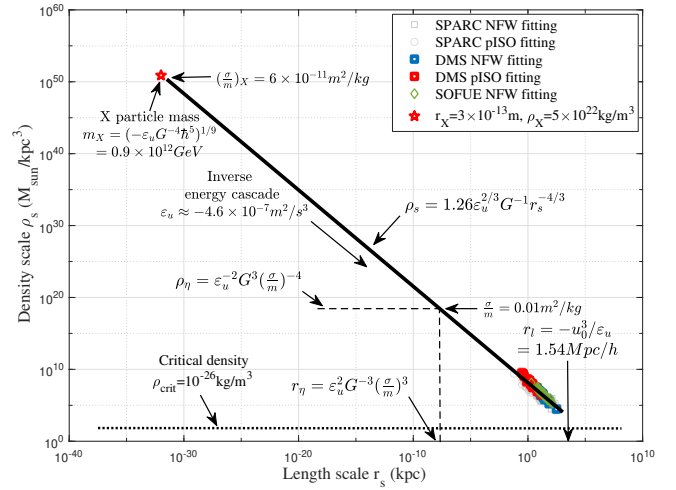


Figure 8. For fully collisionless dark matter, we may extend the predicted -4/3 law in Fig. 6 to the smallest scale where quantum effect can be important (red star). On this scale, dark matter particles properties are determined by three constants: ε_u , G , and Planck constant \hbar [54].

at least one scatter during the age of haloes ($t_{\text{age}} \approx 1/H_0$), i.e. $\rho_r(\sigma/m)v_r t_{\text{age}} = 1$ such that (using Eq. (7))

$$\frac{r_{\text{cmax}}}{\sigma/m} = \varepsilon_u G^{-1} t_{\text{age}} = 10 \text{ kpc} \frac{g}{\text{cm}^2}. \quad (25)$$

For cross-section $\sigma/m = 0.01 \text{ m}^2/\text{kg} = 0.1 \text{ cm}^2/g$ used in SIDM cosmological simulations [32], halo core size is between r_η and the maximum core size $r_{\text{cmax}} \approx 1 \text{ kpc}$. In other words, maximum core size r_{cmax} formed from self-interaction (not any other mechanisms) can be used to identify the cross-section of postulated self-interaction.

In hydrodynamic turbulence, the smallest length scale $\eta = (v^3/\varepsilon)^{1/4}$ [74] is determined by fluid viscosity ν and rate of energy cascade ε . The kinetic energy is injected at large scale and cascaded down to small scales. Below scale η , structures (eddies) are destroyed by viscous force and kinetic energy is dissipated into heat to increase system entropy (Fig. 1). Here ε can be a variable manually controlled or adjusted by the rate of energy injection on large scale. For faster mixing, thinking about stirring the coffee-milk fluid harder (the larger ε), the scale η would be smaller and mixing would be faster due to greater velocity on that scale. However, for dark matter flow in our universe, inverse (NOT direct) energy cascade is required for hierarchical structure formation on large scales. The rate of energy cascade ε_u is a constant on small scales $r < r_l$ that cannot be manually controlled, which should be a fundamental constant relevant to dark matter properties. Finally, for self-interacting dark matter, it should be interesting to identify the smallest and greatest halo core size (r_η and r_{cmax}) to constrain the cross-section using Eqs. (24) and (25).

7 SCALES FOR COLLISIONLESS DARK MATTER

Now let's consider the second option: dark matter is fully collisionless with flat halo core formed by baryonic feedback mechanism. In this scenario, due to the collisionless nature and scale-independence of ε_u , the four-thirds law should extend from galaxy scale to the smallest scale where the quantum effect becomes important (Fig. 8). This extension is more than 30 orders in size, which hopefully allows us to predict the mass, size and properties of dark matter particles (the

X particle) from three basic constants, i.e. ε_u , G , and Planck constant \hbar [54]. Two examples are the critical mass and length scales,

$$m_X \propto \left(-\frac{\varepsilon_u \hbar^5}{G^4} \right)^{\frac{1}{9}} \approx 10^{12} \text{ GeV}, \quad r_X \propto \left(-\frac{G \hbar}{\varepsilon_u} \right)^{\frac{1}{3}} \approx 10^{-13} \text{ m}. \quad (26)$$

If this is true, the constant ε_u might be an intrinsic property of dark matter with a similar origin as Planck constant \hbar for two reasons:

- (i) For fully collisionless dark matter, there exists a unique "symmetry" between position and velocity in phase space. At any given location, collisionless particles can have multiple values of velocity (multi-stream regime). Similarly, particles with same velocity can be found at different locations. This "symmetry" in phase space is not possible for any non-relativistic baryonic matter.
- (ii) Due to the long-rang gravitational interaction, there exist fluctuations (uncertainty) not only in position (\mathbf{x}) and velocity ($\mathbf{v} = \dot{\mathbf{x}}$), but also in acceleration ($\mathbf{a} = \dot{\mathbf{v}}$) [69].

With $\psi(x)$, $\varphi(p)$, and $\mu(a)$ as wave functions for position, momentum, and acceleration, we can write

$$\begin{aligned} \psi(x) &= \frac{1}{\sqrt{2\pi\hbar}} \int_{-\infty}^{\infty} \varphi(p) \cdot e^{ip \cdot x/\hbar} dp, \\ \varphi(p) &= \frac{1}{\sqrt{2\pi\mu_X}} \int_{-\infty}^{\infty} \mu(a) \cdot e^{ia \cdot p/\mu_X} da, \end{aligned} \quad (27)$$

where constant $\mu_X = -m_X \varepsilon_u = 7.44 \times 10^{-22} \text{ kg} \cdot \text{m}^2/\text{s}^3$. An energy scale $\sqrt{\hbar\mu_X} \approx 10^{-9} \text{ eV}$ can be obtained for the possible dark radiation due to dark matter annihilation or decay. Here we have two pairs of conjugate variables: i) position x and momentum p , and ii) momentum p and acceleration a . By following the standard wave mechanics (will not repeat here), two uncertainty principles can be established for fluctuations of position, momentum, and acceleration for collisionless dark matter,

$$\sigma_x \sigma_p \geq \hbar/2 \quad \text{and} \quad \sigma_p \sigma_a \geq \mu_X/2. \quad (28)$$

More experiment data might be required to test this postulation.

8 CONCLUSIONS

Small scale challenges suggest some missing pieces in our current understanding of dark matter. A cascade theory for dark matter flow provides extra insights. The energy cascade with a constant rate ε_u across different scales is a fundamental feature of dark matter flow. N-body simulation suggests a two-thirds law, i.e. the kinetic energy $v_r^2 \propto (\varepsilon_u r)^{2/3}$ on scale r . This is equivalent to a four-thirds law for density on the same scale, i.e. $\rho_r \propto \varepsilon_u^{2/3} G^{-1} r^{-4/3}$, which can be directly confirmed by data from N-body simulations and galaxy rotation curves. By identifying key constants on relevant scales, limiting scales for collisionless (determined by ε_u , G , \hbar) or self-interacting dark matter (by ε_u , G , σ/m) might be obtained. On halo scale, based on the continuity equation, halo density is shown to be closely dependent on the radial flow and mass accretion. The asymptotic density slope $\gamma = -4/3$ can be obtained for fully virialized haloes with a vanishing radial flow. Simulated haloes can have different limiting slopes due to finite radial flow and different rates of mass accretion. The baryonic feedback might enhance the radial flow and flatten the core density. A modified Einasto density profile is proposed accordingly.

DATA AVAILABILITY

Two datasets for this article, i.e. a halo-based and correlation-based statistics of dark matter flow, are available on Zenodo [75, 76], along with the accompanying presentation "A comparative study of dark matter flow & hydrodynamic turbulence and its applications" [40].

References

- [1] P. J. E. Peebles, *ApJ* **284**, 439 (1984).
- [2] D. N. Spergel, L. Verde, H. V. Peiris, E. Komatsu, M. R. Nolta, C. L. Bennett, M. Halpern, G. Hinshaw, N. Jarosik, A. Kogut, M. Limon, S. S. Meyer, L. Page, G. S. Tucker, J. L. Weiland, E. Wollack, and E. L. Wright, *ApJS* **148**, 175 (2003), [arXiv:astro-ph/0302209 \[astro-ph\]](#).
- [3] E. Komatsu, K. M. Smith, J. Dunkley, C. L. Bennett, B. Gold, G. Hinshaw, N. Jarosik, D. Larson, M. R. Nolta, L. Page, D. N. Spergel, M. Halpern, R. S. Hill, A. Kogut, M. Limon, S. S. Meyer, N. Odegard, G. S. Tucker, J. L. Weiland, E. Wollack, and E. L. Wright, *ApJS* **192**, 18 (2011), [arXiv:1001.4538 \[astro-ph.CO\]](#).
- [4] C. S. Frenk and S. D. M. White, *Annalen der Physik* **524**, 507 (2012), [arXiv:1210.0544 \[astro-ph.CO\]](#).
- [5] L. Perivolaropoulos and F. Skara, *New Astronomy Reviews* **95**, 101659 (2022).
- [6] J. S. Bullock and M. Boylan-Kolchin, *ARA&A* **55**, 343 (2017), [arXiv:1707.04256 \[astro-ph.CO\]](#).
- [7] R. A. Flores and J. R. Primack, *ApJ* **427**, L1 (1994), [arXiv:astro-ph/9402004 \[astro-ph\]](#).
- [8] W. J. G. de Blok, *Adv. Astron.* **2010**, 789293 (2010), [arXiv:0910.3538 \[astro-ph.CO\]](#).
- [9] A. Klypin, A. V. Kravtsov, O. Valenzuela, and F. Prada, *The Astrophysical Journal* **522**, 82 (1999).
- [10] B. Moore, S. Ghigna, F. Governato, G. Lake, T. Quinn, J. Stadel, and P. Tozzi, *The Astrophysical Journal* **524**, L19 (1999).
- [11] M. Boylan-Kolchin, J. S. Bullock, and M. Kaplinghat, *Monthly Notices of the Royal Astronomical Society: Letters* **415**, L40 (2011).
- [12] M. Boylan-Kolchin, J. S. Bullock, and M. Kaplinghat, *Monthly Notices of the Royal Astronomical Society* **422**, 1203 (2012), <https://academic.oup.com/mnras/article-pdf/422/2/1203/3464467/mnras0422-1203.pdf>.
- [13] M. Milgrom, *Astrophysical Journal* **270**, 365 (1983).
- [14] S. S. McGaugh, J. M. Schombert, G. D. Bothun, and W. J. G. de Blok, *Astrophysical Journal* **533**, L99 (2000).
- [15] B. Famaey and S. McGaugh, in *Journal of Physics Conference Series*, Journal of Physics Conference Series, Vol. 437 (2013) p. 012001, [arXiv:1301.0623 \[astro-ph.CO\]](#).
- [16] S. Garrison-Kimmel, M. Boylan-Kolchin, J. S. Bullock, and E. N. Kirby, *Monthly Notices of the Royal Astronomical Society* **444**, 222 (2014), <https://academic.oup.com/mnras/article-pdf/444/1/222/18506913/stu1477.pdf>.
- [17] A. Del Popolo, J. A. S. Lima, J. C. Fabris, and D. C. Rodrigues, *J. Cosmology Astropart. Phys.* **2014**, 021 (2014), [arXiv:1404.3674 \[astro-ph.CO\]](#).
- [18] W. J. G. de Blok and A. Bosma, *A&A* **385**, 816 (2002), [arXiv:astro-ph/0201276 \[astro-ph\]](#).
- [19] W. J. G. de Blok, A. Bosma, and S. McGaugh, *Monthly Notices of the Royal Astronomical Society* **340**, 657 (2003), <https://academic.oup.com/mnras/article-pdf/340/2/657/18649385/340-2-657.pdf>.

- [20] R. A. Swaters, B. F. Madore, F. C. van den Bosch, and M. Balcells, *Astrophys. J.* **583**, 732 (2003), [arXiv:astro-ph/0210152](#).
- [21] R. Kuzio de Naray and T. Kaufmann, *Monthly Notices of the Royal Astronomical Society* **414**, 3617 (2011), <https://academic.oup.com/mnras/article-pdf/414/4/3617/18715139/mnras0414-3617.pdf>.
- [22] J. F. Navarro, C. S. Frenk, and S. D. M. White, *Astrophysical Journal* **490**, 493 (1997).
- [23] J. F. Navarro, A. Ludlow, V. Springel, J. Wang, M. Vogelsberger, S. D. M. White, A. Jenkins, C. S. Frenk, and A. Helmi, *Monthly Notices of the Royal Astronomical Society* **402**, 21 (2010), <https://academic.oup.com/mnras/article-pdf/402/1/21/18573804/mnras0402-0021.pdf>.
- [24] J. Diemand and B. Moore, *Advanced Science Letters* **4**, 297 (2011), [arXiv:0906.4340 \[astro-ph.CO\]](#).
- [25] F. Governato, C. Brook, L. Mayer, A. Brooks, G. Rhee, J. Wadsley, P. Jonsson, B. Willman, G. Stinson, T. Quinn, and P. Madau, *Nature* **463**, 203 (2010).
- [26] D. McKeown, J. S. Bullock, F. J. Mercado, Z. Hafen, M. Boylan-Kolchin, A. Wetzel, L. Necib, P. F. Hopkins, and S. Yu, *MNRAS* **513**, 55 (2022), [arXiv:2111.03076 \[astro-ph.GA\]](#).
- [27] A. Del Popolo and M. Le Delliou, *Galaxies* **5**, 17 (2017), [arXiv:1606.07790 \[astro-ph.CO\]](#).
- [28] J. F. Navarro, V. R. Eke, and C. S. Frenk, *MNRAS* **283**, L72 (1996), [arXiv:astro-ph/9610187 \[astro-ph\]](#).
- [29] S.-H. Oh, C. Brook, F. Governato, E. Brinks, L. Mayer, W. J. G. de Blok, A. Brooks, and F. Walter, *AJ* **142**, 24 (2011), [arXiv:1011.2777 \[astro-ph.CO\]](#).
- [30] A. Benítez-Llambay, C. S. Frenk, A. D. Ludlow, and J. F. Navarro, *Monthly Notices of the Royal Astronomical Society* **488**, 2387 (2019), <https://academic.oup.com/mnras/article-pdf/488/2/2387/28979701/stz1890.pdf>.
- [31] D. N. Spergel and P. J. Steinhardt, *Phys. Rev. Lett.* **84**, 3760 (2000).
- [32] M. Rocha, A. H. G. Peter, J. S. Bullock, M. Kaplinghat, S. Garrison-Kimmel, J. Oñorbe, and L. A. Moustakas, *Monthly Notices of the Royal Astronomical Society* **430**, 81 (2013), <https://academic.oup.com/mnras/article-pdf/430/1/81/3064615/sts514.pdf>.
- [33] A. H. G. Peter, M. Rocha, J. S. Bullock, and M. Kaplinghat, *MNRAS* **430**, 105 (2013), [arXiv:1208.3026 \[astro-ph.CO\]](#).
- [34] V. C. Rubin and W. K. Ford, *Astrophysical Journal* **159**, 379 (1970).
- [35] V. C. Rubin, W. K. Ford, and N. Thonnard, *Astrophysical Journal* **238**, 471 (1980).
- [36] G. I. Taylor, *Proceedings of the royal society A* **151**, 421 (1935).
- [37] T. de Karman and L. Howarth, *Proceedings of the Royal Society of London Series a-Mathematical and Physical Sciences* **164**, 0192 (1938).
- [38] G. K. Batchelor, *The Theory of Homogeneous Turbulence* (Cambridge University Press, Cambridge, UK, 1953).
- [39] L. F. Richardson, *Weather Prediction by Numerical Process* (Cambridge University Press, Cambridge, UK, 1922).
- [40] Z. Xu, “A comparative study of dark matter flow & hydrodynamic turbulence and its applications,” (2022).
- [41] Z. Xu, [arXiv e-prints](#), [arXiv:2109.09985](#) (2021).
- [42] Z. Xu, [arXiv e-prints](#), [arXiv:2110.13885](#) (2021).
- [43] Z. Xu, *Physics of Fluids* **35**, 077105 (2023), [arXiv:2202.00910 \[astro-ph\]](#).
- [44] Z. Xu, *A&A* **675**, A92 (2023), [arXiv:2110.03126 \[astro-ph\]](#).
- [45] J. Neyman and E. L. Scott, *Astrophysical Journal* **116**, 144 (1952).
- [46] A. Cooray and R. Sheth, *Physics Reports-Review Section of Physics Letters* **372**, 1 (2002).
- [47] Z. Xu, *Scientific Reports* (2023), [10.1038/s41598-023-42958-6](#), [arXiv:2210.01200 \[astro-ph\]](#).
- [48] P. J. E. Peebles, *The Large-Scale Structure of the Universe* (Princeton University Press, Princeton, NJ, 1980).
- [49] C. S. Frenk, J. M. Colberg, H. M. P. Couchman, G. Efstathiou, A. E. Evrard, A. Jenkins, T. J. MacFarland, B. Moore, J. A. Peacock, F. R. Pearce, P. A. Thomas, S. D. M. White, and N. Yoshida, [arXiv:astro-ph/0007362v1](#) (2000), [10.48550/arXiv.astro-ph/0007362](#).
- [50] A. Jenkins, C. S. Frenk, F. R. Pearce, P. A. Thomas, J. M. Colberg, S. D. M. White, H. M. P. Couchman, J. A. Peacock, G. Efstathiou, and A. H. Nelson, *Astrophysical Journal* **499**, 20 (1998).
- [51] W. M. Irvine, *Local Irregularities in a Universe Satisfying the Cosmological Principle*, Thesis, HARVARD UNIVERSITY (1961).
- [52] D. Layzer, *Astrophysical Journal* **138**, 174 (1963).
- [53] Z. Xu, [arXiv e-prints](#), [arXiv:2202.04054](#) (2022).
- [54] Z. Xu, [arXiv e-prints](#), [arXiv:2202.07240](#) (2022).
- [55] Z. Xu, [arXiv e-prints](#), [arXiv:2202.06515](#) (2022).
- [56] D. Nelson, A. Pillepich, S. Genel, M. Vogelsberger, V. Springel, P. Torrey, V. Rodriguez-Gomez, D. Sijacki, G. Snyder, B. Griffen, F. Marinacci, L. Blecha, L. Sales, D. Xu, and L. Hernquist, *Astronomy and Computing* **13**, 12 (2015).
- [57] D. H. Zhao, Y. P. Jing, H. J. Mo, and G. Börner, *Astrophysical Journal* **707**, 354 (2009).
- [58] H. Mo, F. van den Bosch, and S. White, *Galaxy formation and evolution* (Cambridge University Press, Cambridge, 2010).
- [59] T. K. Chan, D. Kereš, J. Oñorbe, P. F. Hopkins, A. L. Muratov, C.-A. Faucher-Giguère, and E. Quataert, *Monthly Notices of the Royal Astronomical Society* **454**, 2981 (2015), <https://academic.oup.com/mnras/article-pdf/454/3/2981/4038253/stv2165.pdf>.
- [60] F. Lelli, S. S. McGaugh, and J. M. Schombert, *AJ* **152**, 157 (2016), [arXiv:1606.09251 \[astro-ph.GA\]](#).
- [61] P. Li, F. Lelli, S. McGaugh, and J. Schombert, *ApJS* **247**, 31 (2020), [arXiv:2001.10538 \[astro-ph.GA\]](#).
- [62] T. P. K. Martinsson, M. A. W. Verheijen, K. B. Westfall, M. A. Bershadsky, D. R. Andersen, and R. A. Swaters, *A&A* **557**, A131 (2013), [arXiv:1308.0336 \[astro-ph.CO\]](#).
- [63] Y. Sofue, *Publications of the Astronomical Society of Japan* **68** (2016), [10.1093/pasj/psv103](#).
- [64] L. Wang and D.-M. Chen, *Research in Astronomy and Astrophysics* **21**, 271 (2021).
- [65] J. Kormendy and K. C. Freeman, in *Proc. IAU Symp. 220, Dark Matter in Galaxies. Astron. Soc. Pac., San Francisco*, edited by W. M. A. Ryder S. D., Pisano D. J. (2004) p. 377.
- [66] M. Spano, M. Marcellin, P. Amram, C. Carignan, B. Epinat, and O. Hernandez, *Monthly Notices of the Royal Astronomical Society* **383**, 297 (2008), <https://academic.oup.com/mnras/article-pdf/383/1/297/3693757/mnras0383-0297.pdf>.
- [67] E. I. Barnes, J. A. Sellwood, and A. Kosowsky, *AJ* **128**, 2724 (2004), [arXiv:astro-ph/0409239 \[astro-ph\]](#).
- [68] M. H. Chan, *Monthly Notices of the Royal Astronomical Society: Letters* **442**, L14 (2014), <https://academic.oup.com/mnras/article->

- [pdf/442/1/L14/9371164/slu047.pdf](#) .
- [69] Z. Xu, [arXiv e-prints](#) , [arXiv:2203.05606](#) (2022).
 - [70] M. Markevitch, A. H. Gonzalez, D. Clowe, A. Vikhlinin, W. Forman, C. Jones, S. Murray, and W. Tucker, *The Astrophysical Journal* **606**, 819 (2004).
 - [71] M. Bradač, S. W. Allen, T. Treu, H. Ebeling, R. Massey, R. G. Morris, A. von der Linden, and D. Applegate, *ApJ* **687**, 959 (2008), [arXiv:0806.2320 \[astro-ph\]](#) .
 - [72] W. A. Dawson, D. Wittman, M. J. Jee, P. Gee, J. P. Hughes, J. A. Tyson, S. Schmidt, P. Thorman, M. Bradač, S. Miyazaki, B. Lemaux, Y. Utsumi, and V. E. Margoniner, *ApJ* **747**, L42 (2012), [arXiv:1110.4391 \[astro-ph.CO\]](#) .
 - [73] A. Robertson, R. Massey, and V. Eke, *Monthly Notices of the Royal Astronomical Society* **465**, 569 (2016), <https://academic.oup.com/mnras/article-pdf/465/1/569/8593057/stw2670.pdf> .
 - [74] A. N. Kolmogoroff, *Comptes Rendus De L Academie Des Sciences De L Urss* **32**, 16 (1941).
 - [75] Z. Xu, “Dark matter flow dataset part i: Halo-based statistics from cosmological n-body simulation,” (2022).
 - [76] Z. Xu, “Dark matter flow dataset part ii: Correlation-based statistics from cosmological n-body simulation,” (2022).